
RADIATION MONITORING SYSTEM FOR LHCb INNER TRACKER

V.M. PUGATCH, Y.V. PYLYPCHENKO, O.YU. OKHRIMENKO,
V.M. IAKOVENKO, V.O. KYVA, M.S. BORYSOVA,
O.S. KOVALCHUK, O.V. MYKHAYLENKO

UDC 621.38
© 2009

Institute for Nuclear Research, Nat. Acad. of Sci. of Ukraine
(47, Nauky Ave., Kyiv 03680, Ukraine)

Performance requirements to and the design of a radiation monitoring system (RMS) for the LHCb Inner Tracker (CERN) have been presented. The physical principle of operation and some constructional details of metal foil detectors (MFDs) developed at the Institute for Nuclear Research of the National Academy of Sciences of Ukraine and used in the RMS manufacture have been described. The results of a testing demonstrate that the parameters of the RMS correspond to the requirements of the LHCb experiment.

should be stored in order that the functioning of the systems aimed at maintaining the operation of silicon microstrip detectors could be corrected adequately [4]. Just this task is the main destination of the radiation monitoring system (RMS) described in this work. The data measured by the RMS are to be transmitted to the control panels of the LHC accelerating complex and the LHCb experiment.

1. Introduction

The LHCb (Large Hadron Collider beauty) is one of four experiments designed for the LHC (Large Hadron Collider). The main purpose of this experiment is a precise study of CP-parity violation in decays of B-mesons, as well as the study of their rare decay channels. To achieve it, a unique system is required for the identification of tracks of those particles which are the product of B-meson decay. The experimental track system consists of a vertex detector (VD) and external tracker (ET), as well as inner (IT) and trigger (TT) silicon trackers [1].

Particle fluxes that are expected in the LHCb experiment [2, 3] are high enough even at the nominal luminosity (an integral exposure dose of about 60 kGy) to exert a substantial influence on the operation of silicon microstrip sensors of LHCb internal trackers [1] and register electronics. Therefore, the radiation load has to be monitored in order to exclude a destruction of expensive experimental facilities. The absorbed dose should be measured “on-line” and the measured data

2. Metal Foil Detectors for Radiation Monitoring

Various methods applied to monitor radiation loads include the monitoring of sensor currents, the *p*-MOSFET dosimetry, the measurement of induced radioactivity in aluminum foils, and so on [5]. The metal foil detector (MFD) technology has been selected for the creation of RMS IT [6] as such that possesses a number of advantages and meets the requirements discussed above [3, 7].

The principle of MFD operation is demonstrated in Fig. 1. Fast charged particles, when passing through a metal foil, generate the electron emission from its surface layers (10 to 50 nm in thickness). This process is known as secondary electron emission (SEE) [8–10]. Electron emission gives rise to the formation of a positive charge on the foil. This charge is integrated by charge-sensitive integrators connected with the metal foil (Fig. 1). The first SEE monitor was tested in 1955 [11]; however, there were no charge integrators sensitive enough at that time.

The properties of SEE essential for the MFD to operate are as follows:

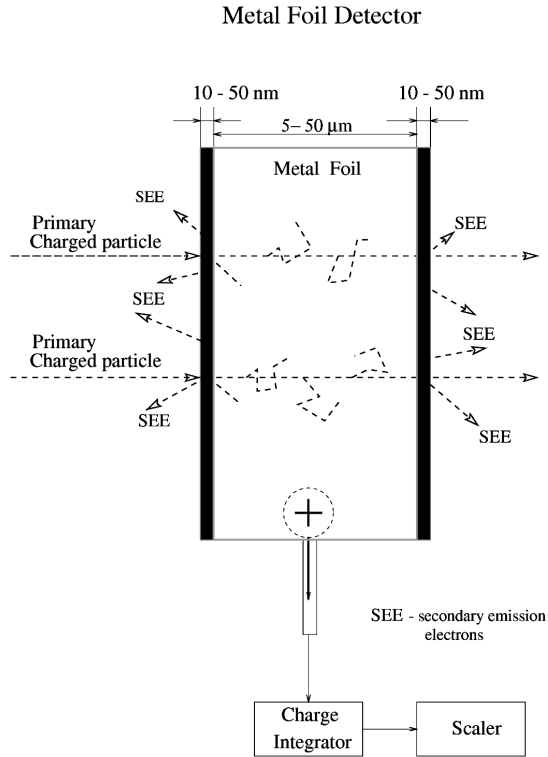


Fig. 1. Mechanism of metal foil detector functioning

– The flux of secondary electrons from a foil made up of a specific material is proportional to the energy loss of a particle that passes through the foil. The number of secondary electrons per one primary particle changes from 0.1 to several hundreds of electrons.

– The main contribution to SEE is given by a few atomic layers located on both foil sides. The SEE flux is almost independent of the foil thickness, if the foil is thicker than several microns. For instance, the flux of secondary electrons saturates already at a thickness of about 5 nm and reaches four, on the average, electrons per α -particle with an energy of 3 MeV [12].

– The energy distribution of SEE has a peak in the range of several eV. The electron spectrum contains contributions from Auger and δ -electrons. The integral contribution of SEE dominates with a factor of 10.

– For pure metals, the flux of secondary electrons does not depend considerably on the metal temperature. The SEE-based sensors are radiation-resistant. The SEE flux was demonstrated to remain constant at bombarding up to a dose of 10^{20} protons/cm². The stable work of SEE-based monitors was observed up to a beam density of $150 \mu\text{A}/\text{cm}^2$, which corresponds to a charged particle flux of $10^{15} \text{ cm}^{-2} \times \text{s}^{-1}$ [13].

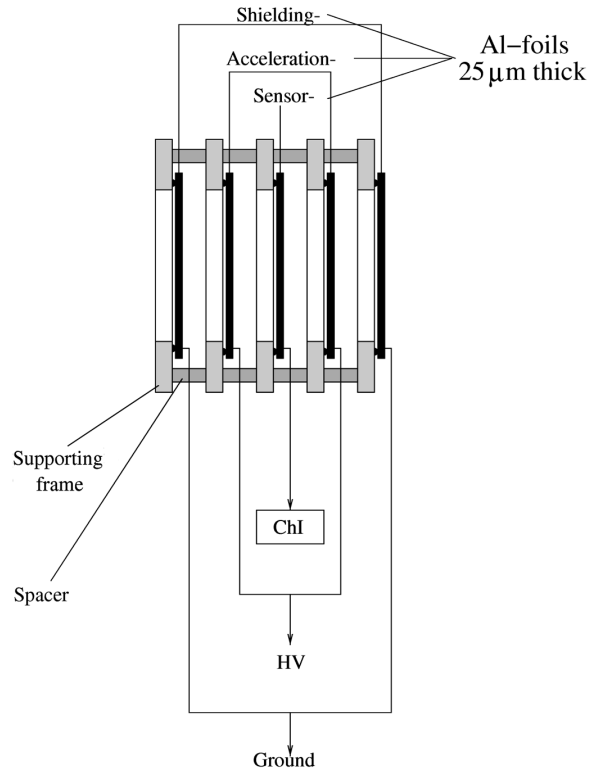


Fig. 2. Scheme of MFD components

In combination with the microstrip technology, the MFD is the thinnest detector that has ever been created for monitoring the fluxes of high-energy particles [14]. As a real device, the MFD is a 5-layer structure (see Fig. 2). Thin metal foils, usually $10\text{--}50 \mu\text{m}$ in thickness, are glued to a dielectric frame – for instance, a 0.5-mm epoxy wafer. To stabilize the MFD operation, auxiliary foils (two accelerating and two screening ones) are located on both sides of the sensor.

The charge that emerges in the sensor is measured with a sensitive charge integrator (CI) [15]. The accelerating voltage (HV), which is required to saturate the MFD response, is about 10–20 V, provided that the distance between the foils is shorter than 3 mm. Such a magnitude is a result of the dominant contribution made by low-energy electrons at SEE [8]. The signal generated by the MFD is approximately 5 times larger in comparison with that generated by a single-layer detector [16].

The MFD possesses a number of advantages which stimulate us to make a choice in its favor for the RMS:

– a possibility to provide a very small amount of detecting material (practically, several tens of microns);

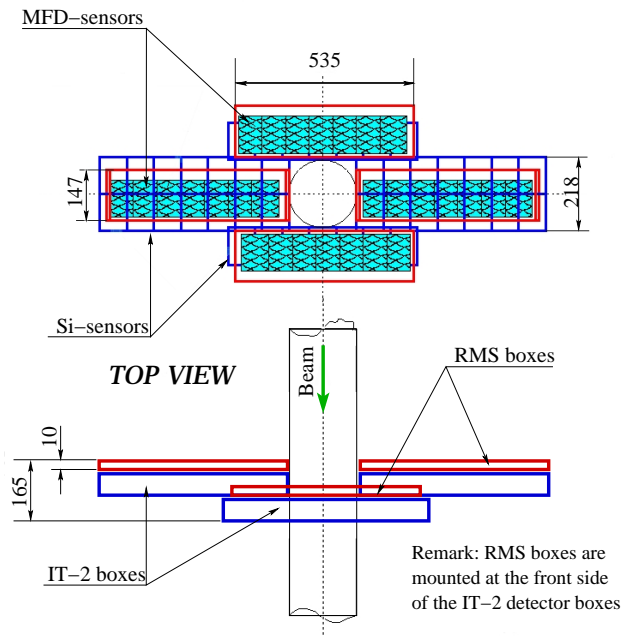


Fig. 3. Schematic front view (above) and view from above (below) of the RMS for the LHCb inner tracker at the IT-2 station

- a simple design at any shapes and dimensions (thin metal foils supported by a dielectric frame);
- low operating voltage;
- simple register electronics (a charge integrator and a counter);
- high radiation resistance;
- long-term operating capacity with a minimal maintenance service;
- low price.

MFDs proved their reliability for the radiation monitoring of charged particles in a wide scope of applications [16].

3. Requirements to RMS Technical Characteristics

The main requirements to the RMS are as follows:

- The distribution of a charged particle flux through silicon sensors of the inner tracker at the IT-2 station has to be permanently measured during 10 years with an accuracy not worse than 10%.
- Information from the RMS has to be transmitted on-line to the LHCb and LHC control panels, with the messages “Warning” and “Radiation hazard” having the highest priority.
- On-line display of radiation conditions and off-line recording of data to be analyzed.

The flux of charged hadrons [2, 3] in the region, where the silicon sensors of the IT-2 station are located, varies from 10^4 to 10^5 $\text{cm}^{-2} \times \text{s}^{-1}$ at the LHCb nominal luminosity of 2×10^{32} $\text{cm}^{-2} \times \text{s}^{-1}$, which corresponds to a pp -interaction frequency of 16 MHz. According to those conditions, the total flux through silicon sensors (11×7.8 cm^2) ranges from 8×10^5 to 2×10^7 s^{-1} . Such magnitudes of hadron flux falls within the dynamic range from 5×10^3 to 5×10^8 s^{-1} of the developed RMS IT (see Section 6.). The MFD technology provides a stable response during a long-term operation with fluctuations within the limits of several percent [16, 17].

The RMS design should include the minimal amount of a constructional material and, at the same time, preserve the mechanical strength of the entire construction and prevent noises of various kinds.

4. RMS IT Design

The RMS will be located at the IT-2 station of the inner tracker, where the space of about 10 mm along the axis of proton beam is allocated for this purpose (Fig. 3). Each of the four identical modules contains seven MFD sensors; they will be fixed on the front side of the IT-2 station detectors. The MFD sensors of the upper and lower RMSs will reproduce approximately the shape of silicon sensors, being displaced upward a little with respect to the detector boxes of the IT-2 station. The MFD sensors of the modules on the left and on the right (Fig. 3.) will cover only half the area of silicon sensors. It should suffice for the approximate estimation of the absorbed dose over the whole area of silicon sensors.

The scheme of an RMS module for the IT-2 station is depicted in Fig. 4. The supporting wafer (535×147 cm^2) 0.05 mm in thickness is fabricated of the G10 material (fiber glass impregnated with epoxy resin). The apertures in the wafer are used to regulate and to fix the RMS module on the surface of detector boxes of the IT-2 station. Seven sensors are gripped between thin frames. The frames 0.05 mm in thickness are fabricated of the G10 material; their edges are 2–3 mm in thickness; the frame windows correspond to the dimensions of an MFD sensor (110×75 mm^2). The sensor layer is surrounded by the accelerating and screening layers made up of aluminum foils 25 μm in thickness; the foils are also gripped between the frames (Fig. 3). The supporting wafer and the frames provide a design necessary for the 5-layer construction to be mechanically rigid.

A dielectric grid 100 μm in thickness is located between auxiliary aluminum layers (Fig. 4). It is fabricated from polypropylene fibers 1 and 0.25 mm in

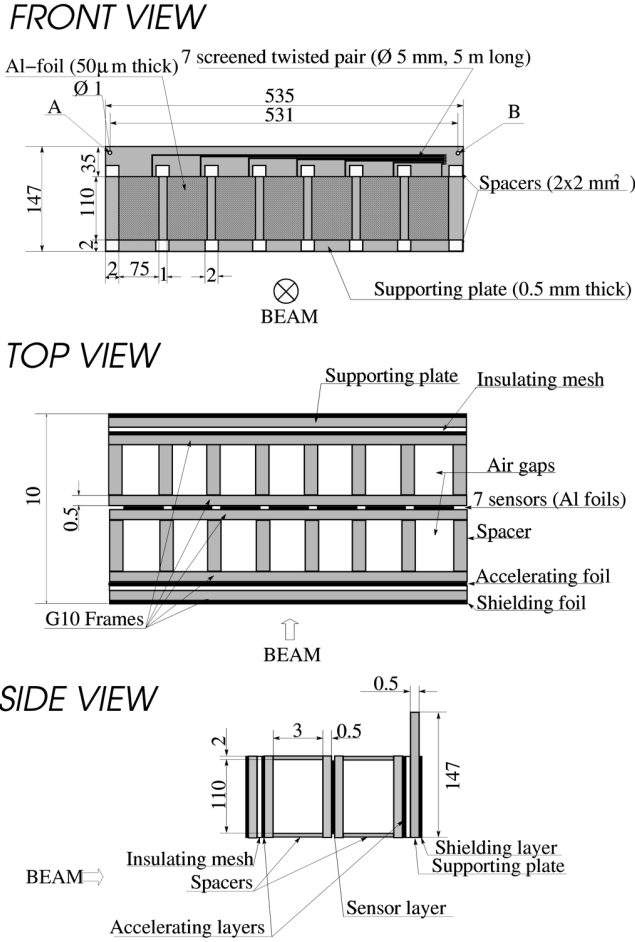


Fig. 4. Scheme of an RMS module for the LHCb inner tracker (no scale)

thickness. In total, there are two polypropylene grid layers, which contribute 0.01% of the material—in terms of radiation length—to the detector region (see the Table). Sixteen epoxy spacers ($2 \times 2 \text{ mm}^2$ in area and 3 mm in thickness) are inserted between the sensor and each accelerating layer in order to ensure their spatial separation. The spacers cover less than 0.1% of the total module area.

The ground circuit is exhibited in Fig. 5. The screening layers are connected to the ground of CIs through the cable winding. RC-filters used for the stabilization of the running voltage are located at a distance of 5 m, in a patch panel.

Figure 6 and the Table give an estimation for the contribution of the RMS-module material in terms of the radiation length.

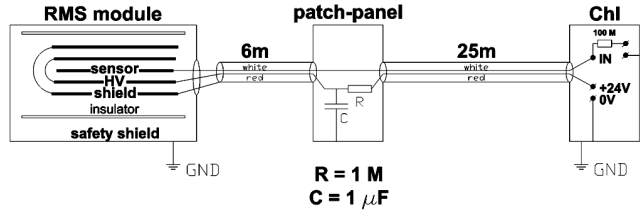


Fig. 5. Ground circuit of the RMS module

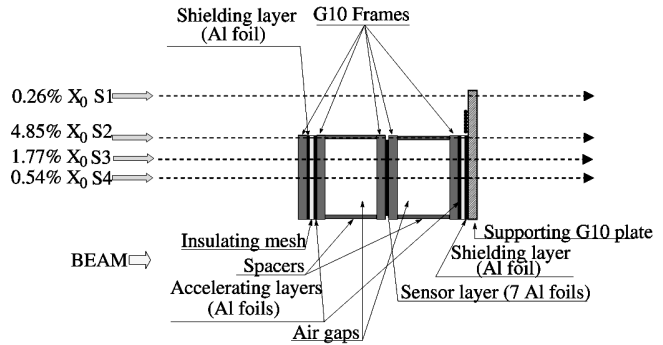


Fig. 6. Contributions of the RMS module materials for directions S1, S2, S3, and S4 (in terms of the radiation length X_0)

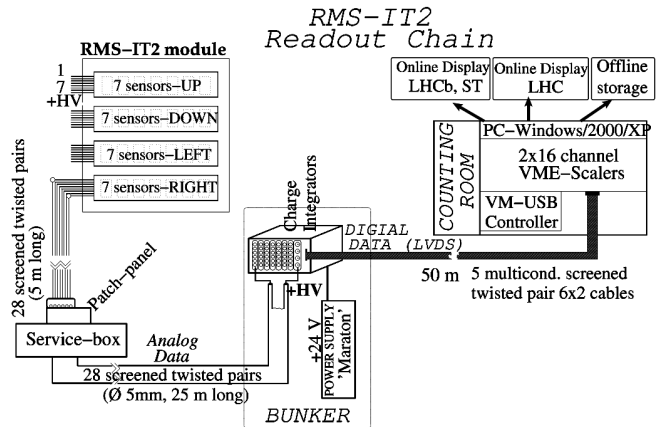


Fig. 7. System of readout from the RMS IT in the LHCb experiment

5. Readout Electronics and Software for RMS

Requirements to the long-term characteristics and the reliability of RMS should provide a simple fast accumulation of data, as well as a permanent calibration. The scheme of the RMS readout circuit is presented in Fig. 7. An analog signal from 28 sensors is read out by sensitive CIs. To read out the signal, 28 screened twisted pairs – each 5 m in length and 5 mm in diameter – are used: one wire (white) is used for the signal transmission, the other (red) for supplying the accelerating voltage

(24 V). These cables are stuck to the foils and the supporting wafer making use of the silver and epoxy glues, respectively (see also Fig. 4). These cables are used to transmit the signal from sensors at the IT-2 station to charge integrators in the bunker through the patch panel, where the RC-filters are located.

The charge-to-frequency converter was developed at the Institute for Nuclear Research (Kyiv) [15, 18]. It was improved at the MPIfK (Heidelberg) and used in the HERA-B experiment to monitor the interaction frequency and the beam profile [17]. Charge integrators used in the HERA-B experiment did not change their properties after having been irradiated up to doses of 2–3 krad. The total exposure dose, which is expected to be in the LHCb bunker for 10 years of the accelerator functioning, will not exceed several hundreds of rads.

The converter is based on a recirculating charge integrator with auto startup and a restore circuit. It transforms an input charge into a sequence of output pulses, whose frequency F_{out} is proportional to the input current I_{in} and reciprocal to the integrating capacity C_i and the discriminator threshold difference $\Delta U = U_H - U_L$:

$$F_{out} = I_{in}/(C_i\Delta U). \tag{1}$$

The input current with positive polarity is integrated by an integrator, the output voltage of which, U_{out} , falls down to the lower discriminator threshold U_L . At the discriminator actuation moment, the discharge current switches on, and the voltage U_{out} starts to grow. When the upper discriminator threshold U_H is achieved, the discharge current switches off, and a new cycle of integration begins. Further, the process repeats. The output shaper forms a signal with output frequency in the NIM and TTL standards.

The signal from a sensor is amplified by an operational amplifier on field transistors (IC19, OPA602) and, then, integrated by the next cascade (IC20), where a precise low-noise operational amplifier (OPA37) is used. The next cascade (IC24, VFC110) transforms the voltage into the frequency, following the principle described above. The output cascade (IC21, MC01024, 74HC08) is used to provide NIM/TTL-standards of the output signal. The measurements of the base line is carried out by supplying the base current, which is fixed now at the level of 24 pA and ensures the output signal frequency of 25 kHz, to the charge integrator input. The conversion factor of the charge integrator is 1 kHz per 1 pA of the input current (the fluctuations of output signals do not exceed several Hz). The linearity of a charge integrator is better than 0.02% for input currents within the interval from 1 to 1000 pA. The temporal instability during 24 h is $\pm 0.05\%$, and the temperature instability is lower than 0.1% per 1 °C.

Five charge integrators are arranged in the same NIM-block. The crate contains seven NIM-blocks (35 charge integrators) in total. The crate is supplied by the voltages of ± 24 V (1 A) and ± 6 V (1.5 A) from a MARATON power source which is located in the bunker of the LHCb experiment. The accelerating voltage of +24 V, which is required for the MFD to work, is generated by the same power source and filtered by an RC-circuit located in the patch panel.

The output signal from a charge integrator (the TTL-signal) is converted into an LVDS-signal and transmitted through a 65-m cable (multiline screened twisted pair) to a computer center with two 16-channel VME-counters. The control of and the readout from the VME-counter are carried out by a WIENER VM-USB VME-controller with a USB-2 interface (8 Mbyte/s).

Contributions of RMS module materials

Direction	Material	Thickness, g/cm ²	Contribution to radiation length X_0 , %	Contribution to total area, %
S1	G10: wafer	0.085	0.26	22.5
	G10: wafer, frames, spacers	1.53	4.63	
S2	Polypropylene: grids	<0.001	$\sim 10^{-3}$	~0.1
	Aluminum: 4 layers	0.054	0.22	
	Total		4.85	
S3	G10: wafer, frames	0.51	1.55	~5
	Polypropylene: grids	<0.001	$\sim 10^{-3}$	
	Aluminum: 4 layers	0.054	0.22	
	Total		1.71	
S4	G10: wafer	0.085	0.26	72.5
	Polypropylene: grids	<0.001	$\sim 10^{-3}$	
	Aluminum: 5 layers	0.0675	0.28	
	Total		0.54	

Making use of the PVSS interface, the data are stored in a PVSS archive, whereas the complete information is stored in the event database. The data obtained from the RMS are displayed on-line at the LHCb and LHC control panels.

The trigger is used for the simultaneous startup of a large number of counters. The “gate-and-delay” generator is used to generate a temporal window and to measure a radiation load upon the sensor in the course of data registering, with and without the beam. These data are stored in various buffers for their subsequent analysis; only the data on luminosity are permanently displayed (every 1 to 10 s) in the LHCb and LHC control rooms. In general, the rate of 5 kB/s is sufficient for data transmission, including the data on asymmetry, which are necessary to monitor the beam position [19].

The graphic interface allows the end user to select the levels of “Nominal Radiation Charge”—“Warning” and “Alarm”, as well as the “Interaction Point” in the predefined limits, in accordance with the nominal frequency of the pp -interaction. The software for RMS IT readout electronics allows one

- to monitor the radiation loads and, hence, the pp -interaction frequency;
- to monitor the pp -interaction point;
- to generate the warning and alarm signals;
- to regulate the period of data acquisition;
- to monitor/to correct the base line of CI and/or the background contribution;
- to subtract the background;
- to present the data on-line;
- to accumulate the data.

6. Results of RMS testing

The MFD-based prototypes and working modules of RMS were mounted and tested at the accelerators at the INR (Kyiv), DESY (Hamburg), MPIfK (Heidelberg), and CERN (Geneva) [16]. Nowadays, charge integrators with the conversion coefficient of 1 kHz per 1 pA are used, and the characteristic fluctuations of their output frequency amount to 1–2 Hz. Deviations of the output frequency of an integrator connected with a sensor by a long cable can grow up to 100 Hz, being stimulated by short noises, radio frequencies, and various background contributions. It was shown that the correction for those factors is possible by measuring the MFD response during the periods of irradiation with particles and between them. It allows the fluxes of charged particles on an MFD sensor to be measured starting from the magnitude of $5 \times 10^3 \text{ s}^{-1}$. The lowest flux of particles

that is expected to flow through a silicon sensor at the IT-2 station is an order of magnitude higher.

6.1. Beam profile monitor for LHCb

To test the MFD, a beam profile monitor (BPM) for a LHCb X7-test-beam was constructed and used in test measurements at CERN in May and November, 2001 [20]. The data obtained demonstrated a perfect agreement with the profile of a beam (a flux of $5.2 \times 10^5 \pi$ -mesons with an energy of 120 GeV every 2.4 s) measured with the help of a multiwire proportional chamber which is regularly used for the BPM at CERN.

6.2. Luminosity measurements in the HERA-B experiment

A prototype, which was most similar to the RMS IT, was used to measure the luminosity in the HERA-B experiment (a beam of protons with an energy of 920 GeV). Twelve MFD sensors were mounted around an ion guide near the output window of the vertex detector system. Figure 8 demonstrates the linear response of MFD to the proton-nucleus interaction frequency measured by a hodoscope within the range below 25 MHz. It corresponds to a flux of charged particles of $5 \times 10^8 \text{ s}^{-1}$ through an MFD sensor. The upper limit of MFD linearity can be elevated by reducing the conversion factor of a charge integrator. Thus, the charge integrator characterized by a lower conversion factor can register the jumps of the interaction frequency up to a level of several GHz (the particle flux up to 10^{10} s^{-1} through a sensor).

One should bear in mind that the NIM-crate with charge integrators, which were used to measure the luminosity and to read out data from HERA-B targets, has been near the interaction area for more than 3 years. No radiation-induced failures of the charge integrators have been detected within this period. The total radiation charge at a distance of 1.5 m from the targets was estimated to be of several kilorads. It is much more than the expected dose in the LHCb bunker for 10 years of its functioning, which is evaluated to be lower than several hundreds of rads.

In the HERA-B experiment, the temporal stability of MFD characteristics was also studied. The upper section of Fig. 9 exhibits the ratio between the frequency of a charge integrator output signal and the proton-nucleus interaction frequency measured by a scintillation hodoscope. The lower section demonstrates a projection

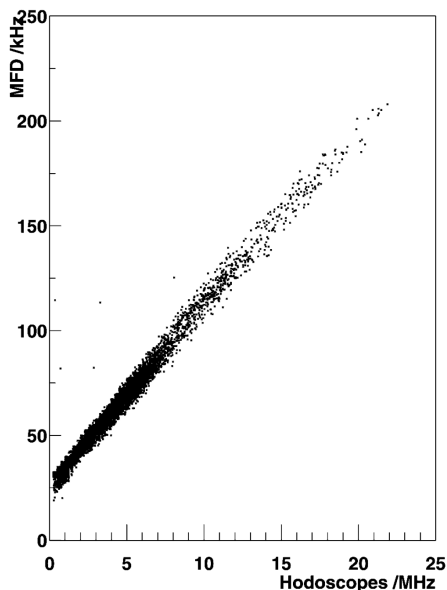


Fig. 8. Dependence of the luminosity monitoring with the help of RMS on the HERA-B interaction frequency measured by a hodoscope

onto the y -axis. Within 2000 h of the permanent MFD work, the signal was stable within an accuracy of 6%. The stability of the base line of a charge integrator (Fig. 9, the middle plot) was better than 0.8%. The minimal flux of charged particles measured making use of the MFD in the HERA-B experiment was estimated as $5 \times 10^3 \text{ s}^{-1}$.

7. RMS Prototype for LHCb Inner Tracker

A number of RMS prototypes were created at the Institute of Nuclear Research of the National Academy of Sciences of Ukraine (Kyiv) to optimize the RMS characteristics and to reduce the amount of a constructional material. In addition to the structures described above, a 7-sensor MFD was constructed in Kiev in 2004, as an RMS prototype for the IT-2 station. The aluminum foil ($25 \mu\text{m}$) of a sensor was glued to a fiber-glass supporting frame which was $550 \times 200 \times 0.1 \text{ cm}^3$ in dimensions and had windows similar to the dimensions of a silicon sensor ($11 \times 7.5 \text{ cm}^2$). The sensor layer was placed between two accelerating foils, and the whole construction was enveloped by grounded foils from both sides.

Additional aluminum foils $25 \mu\text{m}$ in thickness were also glued to a fiber-glass frame which was like a sensor frame. The distance between neighbor layers was 3 mm. To connect sensors with the charge integrator, 5-m

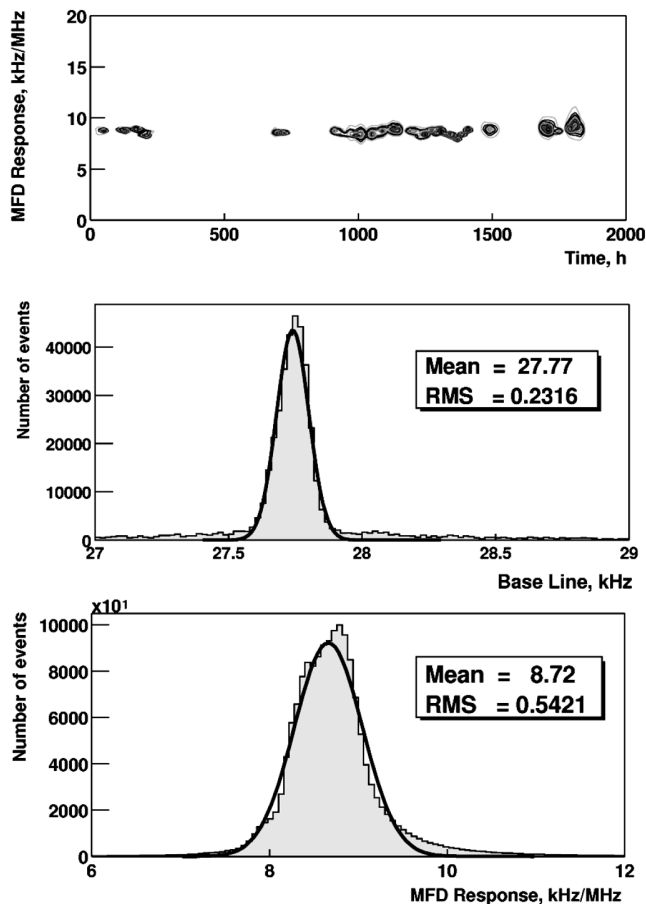


Fig. 9. Characteristics of the MFD prototype for 2000 h

coaxial cables (RG 178) were used. The same cable was used to supply the voltage to the accelerating foils. Data were read out, making use of CAMAC standard blocks, to a personal computer (PC) and stored there for a subsequent analysis. Data were read out by counters every second. To verify that the calibration is correct within the whole period of data accumulation, the base line of each channel from a stable current source was measured permanently.

The characteristics of a RMS prototype were analyzed, by using a ^{90}Sr β -source. The particle flux intensity was about 10^6 s^{-1} per sensor. The differences between sensor responses varied from 4.1 to 8.8 kHz. Such differences were induced by the absorption of low-energy β -particles in a constructional material of supporting frames. The fluctuations of the output frequency of charge integrators varied within the limits of 40–70 Hz.

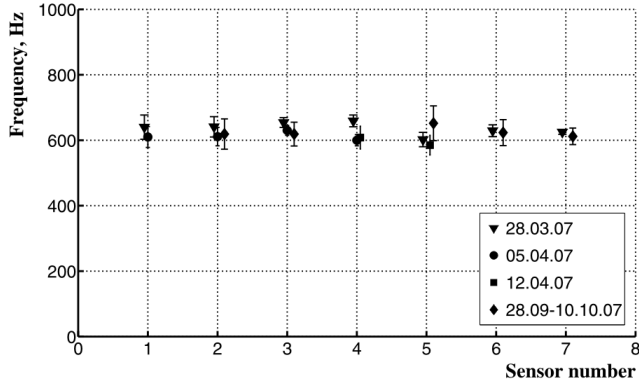


Fig. 10. Time dependence of the RMS response uniformity

We also tested a prototype of the RMS module for the temporal uniformity of its response. The ionizing radiation source and the geometry of the experiment were the same as in the previous researches, i.e. about 10^6 particles/s fell onto a sensor. The scheme of connecting the RMS is similar to that which will be used in the LHCb experiment (Fig. 5). but CIs with a lower conversion factor (100 Hz per 1 pA) are used now, i.e. the system response is 10 times lower and varies from 540 to 720 Hz with a relative error ranging from 1 to 8%. Screened twisted pairs are used to connect the RMS module with the patch panel and the patch panel with the charge integrator.

The measurements were carried out in March-April and September-October, 2007. The corresponding results are depicted in Fig. 10. They testify that the system response does not change within the error limits. From those measurements, we also evaluated the conversion factor of RMS to be 50 secondary electrons per one bombarding particle.

8. Conclusions

Metal foil detectors have been adopted as a basis for the creation of a radiation monitoring system for the LHCb inner tracker. Four RMS modules include 28 aluminum sensors, and they will be mounted at the IT-2 station of the inner tracker. A number of prototypes have been created. Their tests have verified the expected characteristics of MFD-based RMSs. Once calibrated, the RMS can also serve to monitor the LHCb luminosity.

We thank U. Straumann, O. Steinkampf, H. Foss, R. Linder, and other members of the LHCb collaboration

for the sincere discussions, critical remarks, and organizational help.

1. The LHCb Collaboration, LHCb Technical Design Report, CERN/LHCC 2003-030.
2. V. Talanov, LHCb Note 2000-013.
3. M. Siegler *et al.*, LHCb Note 2004-070.
4. V. Pugatch *et al.*, Nuovo Cimento A **112**, 1383 (1999).
5. V. Pugatch, <http://lhc-expt-radmon.web.cern.ch/lhc-expt-radmon>
6. V. Pugatch *et al.*, LHCb Note 2002-067.
7. The LHCb Collaboration, LHCb Inner Tracker Technical Design Report 83, CERN/LHCC 2002-029.
8. E.J. Sternglass, Phys.Rev. **108**, 1 (1957).
9. H. Rothard, K.O. Groeneweld, and J. Kemmler, Springer Tracts in Mod. Phys. **123**, 97 (1992).
10. A. Hasselkamp, Springer Tracts in Mod. Phys. **123**, 1 (1992).
11. G.W. Tautfest and H.R. Fechter, Rev. Sci. Instrum. **26**, 229 (1955).
12. E. Steinbauer *et al.*, Nucl. Instr. Meth. **915**, 164 (2000).
13. V.A. V'yalitsun, I.A. Pridnikov, and I.R. Ryabukhov, Prib. Tekhn. Eksp. **3**, 36 (1967).
14. V. Pugatch *et al.*, Abstracts of the 7-th European Workshop on Beam Diagnostics and Instrumentation for Particle Accelerators (DIPAC), Lyon, France, 6-8 June 2005, abstr. CT02.
15. V. Kyva and N. Tkatch, Sci. Papers Inst. Nucl. Res. **2(4)**, 72 (2001).
16. V. Pugatch *et al.*, Nucl. Instr. Meth. A **535**, 566 (2004).
17. V. Pugatch, HERA-B Note 03-020 (2003).
18. Yu. Vassiliev, Yu. Kozir, V. Medvedev, and V. Pugatch, preprint KINR-83-11 (Kyiv, 1983).
19. C. Hast *et al.*, Nucl. Instr. Meth. A **354**, 224 (1995).
20. T. Glebe, A. Ludwig, V. Pugatch, M. Schmelling, F. Lehner, P. Sievers, O. Steinkampf, U. Straumann, A. Vollhardt, and M. Ziegler, LHCb Note 2002-018.

Received 15.01.08.

Translated from Ukrainian by O.I. Voitenko

СИСТЕМА РАДІАЦІЙНОГО МОНІТОРИНГУ ВНУТРІШНЬОГО ТРЕКЕРА ЕКСПЕРИМЕНТУ ЛНСЬ

*В.М. Пугач, Ю.В. Пилипченко, О.Ю. Охріменко,
В.М. Яковенко, В.О. Кива, М.С. Борисова,
О.С. Ковальчук, О.В. Михайленко*

Резюме

Представлено дизайн та конструкцію системи радіаційного моніторингу (СРМ) для внутрішнього трека експерименту ЛНСЬ (ЦЕРН). Описано фізичний принцип та деякі конструктивні деталі металевих фольгових детекторів, розроблених в ІЯД НАН України та застосованих для виготовлення СРМ. Результати тестування показали відповідність характеристик створеної СРМ технічним вимогам експерименту ЛНСЬ.